

OUR SEARCH FOR AN H-R DIAGRAM OF QUASARS

Jack W. Sulentic,¹ Sebastian Zamfir,¹ Paola Marziani,² and Deborah Dultzin³

RESUMEN

El espacio de parámetros conocido como 4DE1 (Eigenvector 1 en cuatro dimensiones) fue introducido hace siete años en un intento de representar las propiedades espectroscópicas en multifrecuencias de los cuásares. Este espacio de diagnóstico ha demostrado ser el más adecuado para unificar la diversidad de AGN con líneas anchas. Aquí reportamos que el poder de diagnóstico del espacio de parámetros 4DE1 se confirma usando espectros ópticos del SDSS, espectros UV del HST y datos de rayos-X del satélite XMM-Newton. La introducción del concepto de Poblaciones A y B, continua brindándonos una manera útil de entender la diversidad de los cuásares. La gran mayoría de los objetos radio callados son de población A ($\text{FWHM } H\beta \leq 4000 \text{ km s}^{-1}$) y tienen altas tasas de acreción y relativamente bajas masas del agujero negro nuclear. Son potentes emisores de FeII, del llamado exceso en rayos-X suaves, y muestran corrimientos al azul en los perfiles de las líneas de CIV. Los objetos de población B ($\text{FWHM } H\beta > 4000 \text{ km s}^{-1}$) incluyen a la mayoría de los objetos radio fuertes, con mayores masas del agujero negro y bajas tasas de acreción. Éstos muestran débil (o nula) emisión de FeII, del exceso en rayos-X suaves y de corrimientos al azul de las líneas de CIV.

ABSTRACT

The 4D Eigenvector 1 parameter space was introduced seven years ago as an attempt at multiwavelength spectroscopic representation of quasars. It appears to be the most effective diagnostic space for unifying the diversity of broad line AGN. This progress report shows that the diagnostic power of 4DE1 is confirmed using optical spectra from the SDSS, UV spectra from HST and X-ray spectra from XMM-Newton. Our introduction of the population A-B concept continues to provide useful insights into quasar diversity. Largely radio-quiet, high accreting, low BH mass Population A sources ($\text{FWHM } H\beta \leq 4000 \text{ km s}^{-1}$) show strong FeII emission, a soft X-ray excess and a CIV profile blueshift. Low accreting large BH mass Population B quasars ($\text{FWHM } H\beta > 4000 \text{ km s}^{-1}$) include most radio-loud AGN and show weak FeII emission and little evidence for a soft X-ray excess or a CIV blueshift.

Key Words: galaxies: active — quasars: emission lines — quasars: general

1. INTRODUCTION

A NED search for references to one of the hundred brightest AGN (e.g. PG quasars; Boroson & Green 1992, hereafter BG92) will frequently yield ~ 50 – 200 “hits”, but among these one will often find only very few papers dealing with optical/UV spectroscopy of that source. This is surprising especially if one considers that such spectra offer the most direct insights into the geometry and kinematics of the central broad and narrow line regions. Multiwavelength astronomy is apparently still in its infancy with most papers dealing with monochromatic measures. While AGN unification schemes are popular up till recently-no spectroscopic unification has ex-

isted for AGN. This is due to at least two things: (1) until relatively recently few sources with moderate to high resolution and S/N spectroscopy existed for AGN and (2) there has been a common belief that AGN spectra are basically the same. The SDSS has ameliorated the former problem, although caution is required if one considers spectra for sources fainter than $g \sim 17.5$.

We have been searching for a spectroscopic unification embracing all broad line AGN for the past 10+ years. Our hope was to find a diagnostic space that could serve somewhat the same role as the H-R Diagram serves for stellar studies. The H-R Diagram functions well in 2D although its full power requires exploitation of more parameter dimensions. Certainly an equivalent spectroscopic diagnostic space for quasars will require more than two dimensions if only to remove the degeneracy between source physics and line-of-sight orientation – as drivers of measured source properties. This is a problem that

¹Department of Physics & Astronomy, University of Alabama, Tuscaloosa, 35487 USA (giacomo@merlot.astr.ua.edu).

²Osservatorio Astronomico di Padova, 35122 Padova, Italia.

³Instituto de Astronomía, Universidad Nacional Autónoma de México, México.

does not afflict the stellar H-R diagram. In 2000 we proposed a 4D Eigenvector 1 parameter space (Sulentic et al. 2000a,b, hereafter 4DE1) as the optimal vehicle for emphasizing spectroscopic diversity while at the same time contextualizing the diverse types of broad-line emitting sources.

Our 4DE1 parameter space provides a potentially fundamental discrimination between major AGN classes. 4DE1 space (Sulentic et al. 2000a,b) incorporates all of the statistically significant line profile similarities and differences that are currently known. 4DE1 has roots in the Principal Component Analysis (PCA) of the Bright Quasar Sample (Eigenvector 1; BG92) as well as in correlations that emerged from ROSAT (e.g. Wang et al. 1996). 4DE1 as we define it involves BG92 measures: (1) full width half maximum of broad $H\beta$ (FWHM $H\beta$) and (2) equivalent width ratio of optical FeII and broad $H\beta$: $R_{\text{FeII}} = W(\text{FeII})/W(H\beta_{\text{BC}})$. We added (3) a measure of the soft X-ray photon index (Γ_{soft}) and (4) a measure of CIV broad line profile displacement at half maximum ($c(1/2)$) to arrive at our 4DE1 space. Other points of departure from BG92 involve explicit comparison of RQ and RL sources as well as subordination of [OIII] measures (although see Zamanov et al. 2002; Marziani et al. 2003b). Finally, we divide AGN into two populations using a simple division at $\text{FWHM } H\beta_{\text{BC}} = 4000 \text{ km s}^{-1}$ with sources narrower and broader than this value designated populations A and B, respectively. The latter distinction was motivated by the observation that almost all RL sources show $\text{FWHM } H\beta_{\text{BC}} > 4000 \text{ km s}^{-1}$ (Sulentic et al. 2000b). This distinction turns out to be more effective for highlighting spectroscopic differences than the more traditional divisions into: (1) RQ-RL sources and (2) NLSy1-BLSy1 sources defined with $\text{FWHM } H\beta_{\text{BC}} < \text{ and } > 2000 \text{ km s}^{-1}$, respectively.

Adopted 4DE1 key parameters were chosen with the following two requirements in mind: (1) measures that showed large intrinsic variance (Σ) and (2) measures that could be made with high precision (σ). Many/most other spectroscopic measures show correlation in 4DE1 and/or population A-B dichotomy (e.g. optical Balmer line asymmetry, UV SIII]1892/CIII]1909 ratio, hard X-ray spectral index) but do not show large enough variance, or cannot be obtained for large enough numbers of sources with suitable precision, to permit adoption as key parameters (e.g. $\Sigma > 20\sigma$). All line measures involve suitably corrected broad line components (reduction procedures are described in Marziani et al. 1996, 2003a; Sulentic et al. 2007). In simplest terms

the key parameters can be said to measure: (1) the dispersion in (low ionization line) BLR cloud velocities, (2) the relative strengths of FeII and $H\beta$ emission, (3) the strength of a soft X-ray excess and (4) the amplitude of systematic radial motions in (high ionization line) BLR emitting gas. In less simple terms (i.e. more model dependent) we likely have: (1) three or four orthogonal variables sensitive to the Eddington ratio, (2) two or three variables sensitive to source inclination, as well as (3) one variable sensitive to black hole mass (FWHM) and another to nebular physics (n_e : R_{FeII}). Taken together they offer the most direct clues about the geometry and kinematics of the broad line region (BLR).

Source occupation in principal planes of 4DE1 can be found in Sulentic et al. (2000a,b, 2007). These studies have made use of ground based optical spectra for the $H\beta$ region, HST archival FOS/STIS UV spectra for the region of CIV and ROSAT X-ray spectra. We have recently (Zamfir et al., in prep.) exploited the SDSS database which offers major advantages: (1) uniform, high resolution ($\sim 1 \text{ \AA}$) and high S/N spectra for the 300+ brightest quasars and (2) broad wavelength coverage (3000–9000 \AA). Our adopted redshift limit $z = 0.7$ allows measures of $H\beta$ and neighboring lines. This has greatly expanded the number of bright quasars in the magnitude and color range of the PG. It also provides a sample with the proper ratio of RL to RQ sources. Uniform FIRST radio measures allow us to explore the differences between RQ and RL sources with a highly complete ($\sim 80\%$; see Jiang et al. 2007) sample. Figure 1 offers an introduction to the optical plane of 4DE1 in the light of the SDSS era and it is reassuring to note that source occupation confirms our previous work. Similarly we describe preliminary X-ray results that come from the growing XMM-Newton spectroscopic sample. We attempt to summarize here the many insights that 4DE1 offers as a diagnostic space that offers a clearer context in which to interpret individual sources.

(1) 4DE1 makes clear that broad line emitting AGN show a wide range of spectroscopic properties – they are not all alike – the intrinsic dispersion in 4DE1 parameters is much larger than measurement errors. The cross in the upper right corner of Figure 1 indicates typical (median) measurement uncertainties which correspond roughly to 3σ . FWHM $H\beta$ measures range from 1000 (smallest known $\sim 630 \text{ km s}^{-1}$; Grupe et al. 1999) to $\sim 23000 \text{ km s}^{-1}$ in our sample (largest known $\sim 40000 \text{ km s}^{-1}$; Wang et al. 2005, in $H\alpha$) and R_{FeII} measures from 0 to ~ 1.8 (most extreme known $R_{\text{FeII}} \sim 6$; Lipari et al. 1993).

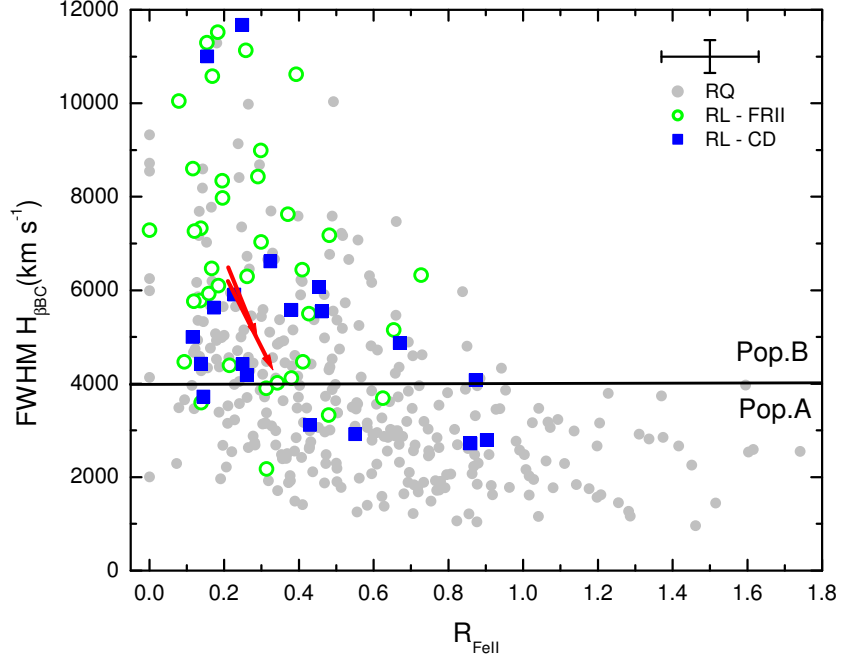


Fig. 1. The SDSS bright quasar sample in the optical plane of 4DE1 space.

Note that SDSS calls sources with $\text{FWHM H}\beta < 1000 \text{ km s}^{-1}$ galaxies rather than quasars and FeII emitters with $R_{\text{FeII}} > 1.8$ were rarely found in the SDSS quasar catalog. They are extremely red objects (strong IRAS sources as well; see Lipari et al. 1993; Véron-Cetty et al. 2006) and they require a special analysis of the FeII emission. These objects are therefore not included in our sample. We regard detection of (broad) FeII emission as a requirement for Type 1 quasar status. Our previous work involved many more sources with R_{FeII} upper limits reflecting the sensitivity of FeII detection to continuum s/n especially for broader line sources (see Marziani et al. 2003a, Figure 3). SDSS spectra for bright quasars reveal less than 1% of broad-line emitting sources with undetected FeII emission suggesting that FeII emission is an ubiquitous property of Type 1 AGN.

Figure 1 tells us that average quasar spectra that do not allow for the wide observed parameter dispersion are somewhat like average stellar spectra involving the entire OBAFGKM sequence (see Sulentic et al. 2002, 2007; Bachev et al. 2004, Zamfir et al., in prep., for average spectra in the 4DE1 context).

(2) Earlier studies (Sulentic et al. 2000a,b) suggested that the RQ majority of AGN showed a larger 4DE1 domain space occupation region than RL sources and this is well confirmed with the SDSS sample. RQ sources (grey filled symbols in Figure 1)

form what can be described as a correlation “main sequence”. There is a large parameter domain where no sources are found. In other words we see a large dispersion in parameter measures but a restricted dispersion in combinations of these measures (e.g. no broad Balmer line profiles [$\text{FWHM H}\beta > 8000 \text{ km s}^{-1}$] with strong FeII emission [$R_{\text{FeII}} > 0.4$]). Narrow Line Seyfert 1 sources (NLSy1) do not emerge as a distinct class but rather as the lower edge of the RQ sequence. If there is a division or dichotomy in source properties it occurs near $\text{FWHM H}\beta = 4000 \text{ km s}^{-1}$.

(3) RL sources (blue filled squares/green open circles) occupy one end of the RQ sequence and overlap with about 25% of RQ sources. This domain space separation is highly significant ($P \sim 3 \times 10^{-7}$ that RQ and RL occupy the same domain; Zamfir et al., in prep.) and credible because we are dealing with unusually complete/balanced RQ and RL samples. These are therefore the only RQ sources that are spectroscopically indistinguishable from RL AGN. We define a source as RL if $\log L_{20\text{cm}}(\text{erg s}^{-1} \text{Hz}^{-1}) = 31.5$ (this is approximately a radio/optical flux density ratio $R_K = 70$; Kellermann et al. 1989). This corresponds to the radio properties of the weakest observed double-lobed (assumed unbeamed in an orientation unification scenario) source in our old and new samples (Sulentic et al. 2003; Zamfir et al., in prep.). The probability of radio loudness in

Figure 1 increases from $P \sim 0.01$ at the extreme RQ end of the source sequence (where NLSy1 are found; Komossa et al. 2006 estimates $P \sim 0.025$ for NLSy1) to $P \sim 0.15$ – 0.18 at the opposite end where the vast majority of RL sources are found.

(4) Few RL sources are found below $\text{FWHM } H\beta_{\text{BC}} = 4000 \text{ km s}^{-1}$. Those that do likely involve sources where the putative accretion disk is seen face-on (and radio jets pole-on) (Sulentic et al. 2003; Zamfir et al., in prep.). We can infer this because we see a separation between the majority of core-dominated sources (CD-filled squares) and lobe-dominated (LD-open circles) emission. Most RL sources with large and small $\text{FWHM } H\beta$ values are lobe- and core-dominated (alternatively steep and flat radio spectrum sources) respectively, again as expected from simple orientation unification schemes (e.g. Urry & Padovani 1995; Orr & Browne 1982) where Balmer emission arises in a flattened cloud distribution (usually called an accretion disk) and the radio-jets are aligned perpendicular to the cloud distribution. Red arrows in Figure 1 indicate the median displacement in 4DE1 optical plane coordinates between FR II and CD sources in the old and new source samples (Sulentic et al. 2003; Zamfir et al., in prep.). This is consistent with LD sources viewed as the (misaligned) parent population of RL sources and with CD sources as the aligned (near pole-on and Doppler boosted) sources. Some CD (largest FWHM) and LD (smallest FWHM) sources do not follow the clear trend indicated by the red arrows in Figure 1. These likely represent the (about 10–15% in our RL sample) “misaligned” sources where the radio jets are far from perpendicular to the accretion disk plane.

(5) All reasonably resolved LD sources in our SDSS sample show FR II morphology suggesting that FR I sources are rare among broad-line RL emitters. Some weak FR I sources may be present among the RQ sources but they show extreme core/lobe ratios and are effectively filtered out of the FIRST survey (dynamic range limits and spatial frequency attenuation). We find no evidence for a significant radio-intermediate population bridging the RQ and RL sources. While weak radio jets are observed in some RQ quasars (e.g. Ulvestad et al. 2005; Leipski et al. 2006), the majority show radio emission dominated by star formation in the host galaxies (e.g. PG quasars follow the radio-FIR correlation; see Haas et al. 2003). There is no evidence for a continuum of radio jet properties from largely LD RL to largely CD RQ sources although a few RQ show unusually strong radio jet-lobe structures (e.g. García-Barreto

et al. 2002). The strongest support for this conclusion comes from 4DE1 (Figure 1) where RL sources show a preferred domain space occupation relative to the RQ majority.

(6) There may be two AGN populations: (1) a “pure” RQ population A which shows little overlap with the RL domain (e.g. it includes $\sim 70\%$ of the RQ sample) and (2) a mixed RL-RQ population B ($\sim 30\%$ of the RQ sources and almost all RL sources). We recently summarized (Sulentic et al. 2007) the empirical (and inferred theoretical differences) between population A and B sources which, in fact, encompass almost all existing multi-wavelength measures of AGN. A recent comparison between FWHM and line dispersion (2nd moment of the profile) measurements for $H\beta$ has accidentally confirmed our two population hypothesis (Collin et al. 2006). Focussing on the key 4DE1 parameters we can say that Population A sources show relatively narrow single-component Balmer lines, strong FeII emission, a CIV blueshift and a soft X-ray excess. Population B sources show broader, and often more complex, Balmer lines, weak FeII emission and absence of a CIV blueshift or soft X-ray excess.

Average Balmer line spectra in the 4DE1 context (Sulentic et al. 2002) require a minimum of two Gaussian components for a reasonable model fit. Aside from the relatively unshifted component assumed to be the “classical” BLR we find a broader and redshifted (VBLR-Very Broad Line Region) component. The latter component is dangerous for reverberation studies and BH mass estimation because it responds to continuum changes differently than the classical BLR (Sulentic et al. 2000c). At the upper extreme of optical 4DE1 space we find a very small number ($< 1\%$) of sources showing double-peaked Balmer line profiles. While they have been interpreted as a direct signature of accretion disk line emission (Eracleous & Halpern 1994) there are many problems with this hypothesis (Sulentic et al. 1999; Sulentic 2006). The situation is reversed for UV high ionization line profiles like CIV1549. Population A sources require unshifted and blueshifted components while population B sources show stronger and less shifted line profiles. Extreme population A sources are sometimes dominated by the blueshifted component.

CIV measures have been clouded in controversy for many years with much of the disagreement centered on the reality and strength of a narrow CIV emission component (Sulentic & Marziani 1999). We recently presented a recipe for reasonable CIV narrow component subtraction (Sulentic et al. 2007) and

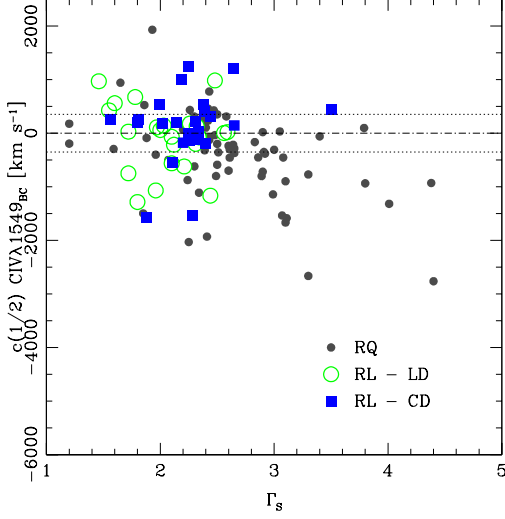


Fig. 2. Our bright quasar sample in a UV – X-ray plane of 4DE1 space. Dashed lines are 2σ confidence intervals for zero CIV shift.

show that corrected broad line measures clarify our picture of high ionization line emission properties in AGN.

(7) Figure 2 shows the current best CIV- Γ_{soft} 4DE1 plane which illustrates two of the population A-B differences summarized above. Figure 2 suggests that population B sources show a much stronger domain space concentration than population A. R_{FeII} and CIV shift ($c(1/2)$) measures also show this concentration. While population A sources show considerable scatter in all 4DE1 measures, population B sources show this scatter only in measures of FWHM $H\beta$. This may be telling us that the physics/geometry/kinematics of population B sources is much more similar from source-to-source. This makes some sense if we view population B sources as the end phase of quasar evolution when the accretion rate is low.

X-ray measures shown in Figure 2 are based largely on archival ROSAT observations. We have only begun to harvest the new generation of XMM-Newton X-ray measures. Three recent papers have analyzed strongly overlapping samples of PG quasars ranging from 20–40 sources (Porquet et al. 2004; Brocksopp et al. 2006; Piconcelli et al. 2005). These samples allow a preliminary test of earlier inferences that motivated us to adopt Γ_{soft} as a key 4DE1 parameter. Table 1 summarizes a comparison of mean XMM-Newton measures for PG quasars observed so far. We restrict this preview to low z PG quasars (included in BG92) for the following two reasons: (1) higher redshift PG sources, assumed to have similar

TABLE 1

Piconcelli-single power-law fit			
Population	N	$\Gamma_{2-12\text{keV}}$	$\Gamma_{0.3-12\text{keV}}$
A	22	1.94	2.71
B	11	1.66	1.88
Pourquet/Brocksopp/Piconcelli-broken power-law fit			
Population	N	Γ_{soft}	Γ_{hard}
A	14/14/13	2.825/2.86/2.98	2.07/2.13/1.39
B	7/6/8	2.31/2.61/2.75	1.795/1.82/1.38

intrinsic X-ray luminosity, will yield lower s/n spectra on average and (2) we have no FWHM $H\beta$ or R_{FeII} measures for higher z PG sources precluding a contextualization in 4DE1 space. We immediately distinguish between our so-called population A and B sources. Even if this distinction turns out not to be fundamental in the sense of physically discrete quasar classes it has proven effective for highlighting differences across the 4DE1 sequence.

The largest difference between population A and B sources involves comparison over the largest energy range (0.3–12keV). The population A-B soft photon index difference is larger than the one reported in the defining papers of the 4DE1 concept (Sulentic et al. 2000a,b). It is also $3\times$ larger than the A-B difference in the “harder” 2–12keV energy range. This was the motivation for suggesting that only population A sources show a soft X-ray excess. XMM-Newton measures confirm the ROSAT derived population A-B difference and Table 1 shows that the mean soft 0.3–12 keV index for population B sources is similar to harder population A-B indices derived over the 0.3–12keV range. Despite claims that all PG quasars show a soft excess, this result suggests that population B source do not.

Single power-law fits to PG X-ray spectra are generally poor which motivated the above studies to consider broken power-laws providing both hard and soft photon indices as given in Table 1. We see some evidence for a stronger population A-B difference in the soft band, however there is considerable variance among the three studies. If we restrict the Brocksopp et al. 2006 sample to broken power-law fits with the best χ^2 solutions we find a soft component population A-B difference $\Delta = 3.0-2.5 \sim 0.5$ which supports a population A soft excess at a K-S significance level $P=0.002$. Sigma values are 0.6 and 0.3 also confirming the smaller scatter among population B sources mentioned above. Clearly we need more X-ray spectra for low z PG quasars.

As also reported earlier (Sulentic et al. 2000a,b) a (smaller) difference is seen for harder X-ray measures in the Piconcelli et al. (2005) sample. Population B sources show a harder spectrum than population A sources in most of the XMM-Newton studies. All three XMM-Newton studies report correlations between FWHM $H\beta$ and soft/hard measures confirming the correlation that we found with a larger ($n=112$) ROSAT sample (Sulentic et al. 2000a,b). The apparently continuous correlation may be telling us that Population A-B are simply the ends of single AGN sequence rather than two distinct classes.

The “soft X-ray excess” has been widely interpreted as the thermal signature of an accretion disk (Pounds et al. 1995). This interpretation is reasonable within the 4DE1 context where the strongest soft excess is found among sources with the smallest black hole masses and highest accretion rates (highest L/L_{Edd}). Following this reasoning Piconcelli et al. (2005) explored composite model fits. It is interesting that models employing a power-law+bremstrahlung yielded a much larger population A-B difference ($kT=0.02$ vs. 0.07) than models employing a power-law+black body. If the population A-B difference is real then this may be telling us that the thermal disk interpretation is incorrect or too simple. Brocksopp et al. (2006) reached a similar conclusion using a different argument. It has been known for a long time that the population A soft excess implies too high temperatures which has motivated some to explore Comptonized disk models (e.g. Haardt et al. 1994).

Two conclusions/comments from the XMM-Newton studies (Piconcelli et al. 2005) require a response within the 4DE1 context. (a) A RL-RQ difference could suggest the presence of an extra continuum contribution from self synchrotron jet emission (Zamorani et al. 1981). 4DE1: We suggest that the few RL sources in PG preclude statistically useful inferences. However in 4DE1 context we know that RQ population B sources show very similar properties to the (largely population B) RL sources. Our much larger ROSAT sample shows this statement to be reasonable. This motivated us to opine that since RQ population B sources show the same spectra as RL sources there is no evidence for an X-ray component related to a source radio-loudness. (b) None of the two component models gives a satisfactory fit for all sources. This result suggests that the shape of the soft excess is not a universal QSO property. 4DE1: The population A-B distinction is very useful here because it suggests that there are two fundamentally different kinds of X-ray emitting quasars.

The soft X-ray excess is only a property of one of these populations.

(8) We recently harvested from the HST archive all UV spectra ($n=130$ sources) covering the CIV $\lambda 1549$ region. We find mean CIV profile shifts (at FWHM) of -677 km s^{-1} and -39 km s^{-1} respectively for population A and B sources confirming the original motivation for adopting this measure as a key 4DE1 parameter (Sulentic et al. 2000b, 2007). The blueshift of high ionization UV emission lines is therefore concentrated in sources with FWHM $H\beta < 4000 \text{ km s}^{-1}$. This means that it is a largely RQ phenomenon (mean CIV profile shifts for RQ and RL sources are -582 km s^{-1} and $+52 \text{ km s}^{-1}$, respectively); CIV equivalent width also shows a striking population A-B difference: 117 \AA and 57 \AA , respectively. We recently discovered an apparent correlation between CIV FWHM and EW measures, but only for population A sources. As mentioned earlier most population B sources show CIV shift/EW, R_{FeII} and Γ_{soft} measures that are identical within measurement uncertainties. We hope to exploit CIV measures as an orientation indicator using this new correlation. It is now well known that the Baldwin effect is dominated by intrinsic (we would say 4DE1) rather than cosmological effects (Bachev et al. 2004; Baskin & Laor 2004).

Physical Inferences: We have described some of the empirical results connected with the four key parameters defining 4DE1 space. 4DE1 is the most effective spectroscopic unifier available, at the same time it emphasizes the differences between AGN. We have also begun to explore the physical implications of 4DE1 (Marziani et al. 2001, 2003b) and suggest the following theoretical inferences from the empiricism; adopting a model where low ionization broad lines (e.g. broad $H\beta$ and FeII emission) arise in a photoionized medium in or near an accretion disk. Simple models then allow us to use: (a) line reverberation to infer the radius of the broad line region (Kaspi et al. 2000, 2005), (b) line FWHM or dispersion to infer the BH mass (assuming a virialized medium: Marziani et al. 2003b; Collin et al. 2006; Sulentic 2006) and (c) R_{FeII} to infer the density of the FeII emitting medium that is as dense as or denser than the region producing $H\beta$ (Marziani et al. 2001, 2008). The Eddington ratio emerges from (b) + source bolometric luminosity. The most useful summary statement here might be a comparison of median inferred properties for population A and B sources. Table 2 summarizes the inferred population A-B values taken from the following papers: Marziani et al. (2001, 2003b); Sulentic (2006). Fig-

TABLE 2

Inferred Physical Properties		
Quantity	Population A	Population B
$\log n_E$	11.5	9.5
$\log U$	-1.5	-1.0
$\log M_{BH}$	7.7	9.0
L/L_{Edd}	0.3	0.08

ure 3 also shows some of the inferred physical trends thought to drive source occupation in the optical plane of 4DE1. See also the review by Marziani (2008).

Collin et al. (2006) recently argued that a thin flat BLR disk structure could be ruled out. We usually assume that $H\beta$, and especially $FeII$, in high accreting population A sources arise in a flatter distribution than population B. This assumption is motivated by empiricism. We can either: (1) compare the typical FWHM $H\beta$ values for the most face-on population A and B sources or (2) the dispersion in observed FWHM values for each population assuming that we observe the BLR over the same range of viewing angles (e.g. 0° to 45°). We also assume that $H\beta$ and $FeII$ emission arise from rather similar cloud distributions because $FWHM FeII \sim FWHM H\beta$. The narrowest population A and B sources show $FWHM H\beta \sim 800 \text{ km s}^{-1}$ and 4000 km s^{-1} , respectively. These are then assumed to be the “face-on” values for the two populations and are measuring motions largely perpendicular to the disk plane where Keplerian rotation dominate. The much smaller velocity dispersion in population A sources is consistent with the idea of a highly flattened distribution. Either population B sources are much less flattened or there is an additional emission component producing the much higher observed velocity dispersion perpendicular to the disk. A more extreme alternative would see line emission in population B sources arising entirely in a non-disk configuration.

Note that the “face-on” value for population A sources is set by the lower limit of observed FWHM $H\beta$ (with $FeII$ emission corroborating that the source is an AGN and that a dense enough medium exists to account for the strong $FeII$ emission). The “edge-on” value of FWHM $H\beta$ for population A is set by the fact that sources with $R_{FeII} > 0.4$ (unambiguously Population A) show $FWHM H\beta < 4000 \text{ km s}^{-1}$. The situation is less confused for population B sources because we can infer the range of FWHM $H\beta$

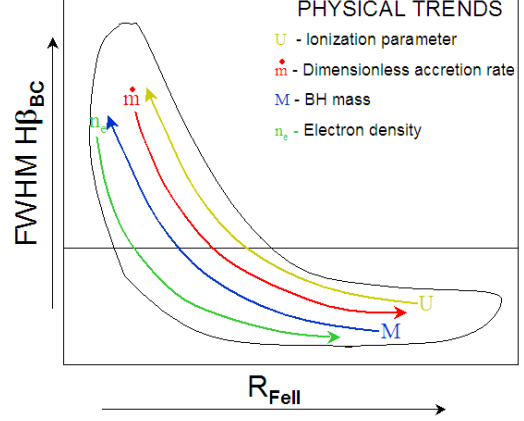


Fig. 3. Inferred physical trends along the quasar sequence in the optical plane of 4DE1 space.

from RL sources via radio morphology and core/lobe flux ratios (Rokaki et al. 2003; Sulentic et al. 2003). We then assume that population B RQ sources follow RL population B because they are co-spatial in 4DE1. Population B sources start to become rare at about $FWHM H\beta = 10^4 \text{ km s}^{-1}$. If we assume the same range of viewing angle for population A and population B sources then we observe velocity ranges of a factor of ~ 5 and ~ 2.5 for population A and B respectively, consistent with a flatter population A emitting cloud distribution.

The typical inferred properties in Table 2 are representative of our current understanding of sources with $z \leq 0.8$. Unfortunately the $H\beta$ spectral region cannot be studied from the ground beyond $z \sim 1.0$ ($z = 0.7$ for SDSS spectra) without major effort. Ground based CIV measures have been extensively used to extract M_{BH} and other properties out to much higher redshift ($z \sim 4.0$). Our own studies of the CIV line using the HST archive suggest that CIV cannot be trusted for M_{BH} estimation for many reasons (Sulentic et al. 2007; Netzer et al. 2007): (1) the obvious Malmquist bias associated with CIV measures for any optically selected sample, (2) the complexity of the CIV profile and properties reflected in population A-B profile differences and the lack of a clear correlation between FWHM $H\beta$ – FWHM (CIV) and (3) especially for the population A (majority) of RQ sources – the blueshifted and blue asymmetric profile shapes which must raise doubts that the high ionization UV lines arise in a virialized medium. Sources with a strong narrow line component (likely more common among population B sources if lines like $[OIII]\lambda 5007$ are any guide) tend to give a false sense of security because

they make CIV profiles look more symmetric and less blueshifted. Recent observations of high z type 2 AGN reveal frequent and reasonable strong CIV narrow line emission (see references in Sulentic et al. 2007).

We have chosen to make a major effort with VLT ISAAC and now have IR spectra of the $H\beta$ region for 50+ sources between $z = 0.8-2.5$. VLT enables us to obtain IR spectra with resolution and s/n similar to ground based spectra for lower redshift sources. Results so far suggest that source occupation in 4DE1 space is similar up to the $B = -29$ to -30 source luminosity range. Much remains to be done but 4DE1 space continues to offer a useful way to contextualize both empirical and physical properties of quasars. It offers the hope of simplifying or resolving many of the current questions about most active objects.

We thank the organizers for the opportunity to speak in Huatulco where we celebrated the birthday of Deborah Dultzin who has been a member of our collaboration for 10+ years.

REFERENCES

- Bachev, R., Marziani, P., Sulentic, J. W., Zamanov, R., Calvani, M., & Dultzin-Hacyan, D. 2004, *ApJ*, 617, 171
- Baskin, A., & Laor, A. 2004, *MNRAS*, 350, L31
- Boroson, T. A., & Green, R. F. 1992, *ApJS*, 80, 109 (BG92)
- Brooksopp, C., Starling, R. L. C., Schady, P., Mason, K. O., Romero-Colmenero, E., & Puchnarewicz, E. M. 2006, *MNRAS*, 366, 953
- Collin, S., Kawaguchi, T., Peterson, B. M., & Vestergaard, M. 2006, *A&A*, 456, 75
- Eracleous, M., & Halpern, J. P. 1994, *ApJS*, 90, 1
- García-Barreto, J. A., Franco, J., & Rudnick, L. 2002, *AJ*, 123, 1913
- Grupe, D., Beuermann, K., Mannheim, K., & Thomas, H.-C. 1999, *A&A*, 350, 805
- Haardt, F., Maraschi, L., & Ghisellini, G. 1994, *ApJ*, 432, L95
- Haas, M., et al. 2003, *A&A*, 402, 87
- Jiang, L., Fan, X., Ivezić, Ž., Richards, G. T., Schneider, D. P., Strauss, M. A., & Kelly, B. C. 2007, *ApJ*, 656, 680
- Kaspi, S., Smith, P. S., Netzer, H., Maoz, D., Jannuzi, B. T., & Giveon, U. 2000, *ApJ*, 533, 631
- Kaspi, S., Maoz, D., Netzer, H., Peterson, B. M., Vestergaard, M., & Jannuzi, B. T. 2005, *ApJ*, 629, 61
- Kellermann, K. I., Sramek, R., Schmidt, M., Shaffer, D. B., & Green, R. 1989, *AJ*, 98, 1195
- Komossa, S., Voges, W., Xu, D., Mathur, S., Adorf, H.-M., Lemson, G., Duschl, W. J., & Grupe, D. 2006 *AJ*, 132, 531
- Leipski, C., Falcke, H., Bennert, N., & Hüttemeister, S. 2006, *A&A*, 455, 161
- Lipari, S., Terlevich, R., & Macchetto, F. 1993, *ApJ*, 406, 451
- Marziani, P., Sulentic, J. W., Dultzin-Hacyan, D., Calvani, M., & Moles, M. 1996, *ApJS*, 104, 37
- Marziani, P., Sulentic, J. W., Zwitter, T., Dultzin-Hacyan, D., & Calvani, M. 2001, *ApJ*, 558, 553
- Marziani, P., Sulentic, J. W., Zamanov, R., Calvani, M., Dultzin-Hacyan, D., Bachev, R., & Zwitter, T. 2003a, *ApJS*, 145, 199
- Marziani, P., Zamanov, R. K., Sulentic, J. W., & Calvani, M. 2003b, *MNRAS*, 345, 1133
- Marziani, P., et al. 2008, *RevMexAA*, 32, 69
- Netzer, H., Lira, P., Trakhtenbrot, B., Shemmer, O., & Cury, I. 2007, *ApJ*, 671, 1256
- Orr, M. J. L., & Browne, I. W. A. 1982, *MNRAS*, 200, 1067
- Piconcelli, E., Jiménez-Bailón, E., Guainazzi, M., Scharrel, N., Rodríguez-Pascual, P. M., & Santos-Lleó, M. 2005, *A&A*, 432, 15
- Porquet, D., Reeves, J. N., O'Brien, P., & Brinkmann, W. 2004, *A&A*, 422, 85
- Pounds, K. A., Done, C., & Osborne, J. P. 1995, *MNRAS*, 277, L5
- Rokaki, E., Lawrence, A., Economou, F., & Mastichiadis, A. 2003, *MNRAS*, 340, 1298
- Sulentic, J. W., Marziani, P., & Dultzin-Hacyan, D. 1999, *ASP Conf. Ser.* 175, Structure and Kinematics of Quasar Broad Line Regions, ed. C. M. Gaskell, W. N. Brandt, M. Dietrich, D. Dultzin-Hacyan, & M. Eracleous (San Francisco: ASP), 175
- Sulentic, J. W., & Marziani, P. 1999, *ApJ*, 518, L9
- Sulentic, J. W., Zwitter, T., Marziani, P., & Dultzin-Hacyan, D. 2000a, *ApJ*, 536L, 5
- Sulentic, J. W., Marziani, P., & Dultzin-Hacyan, D. 2000b, *ARA&A*, 38, 521
- Sulentic, J. W., Marziani, P., Zwitter, T., Dultzin-Hacyan, D., & Calvani, M. 2000c, *ApJ*, 545, L15
- Sulentic, J. W., Marziani, P., Zamanov, R., Bachev, R., Calvani, M., & Dultzin-Hacyan, D. 2002, *ApJ*, 566L, 71
- Sulentic, J. W., Zamfir, S., Marziani, P., Bachev, R., Calvani, M., & Dultzin-Hacyan, D. 2003, *ApJ*, 597, L17
- Sulentic, J. W. 2006, in *Current issues in Cosmology*, ed. J.-C. Pecker & J. Narlikar (Cambridge: Cambridge Univ. Press), 37
- Sulentic, J. W., Bachev, R., Marziani, P., Negrete, C. A., & Dultzin, D. 2007, *ApJ*, 666, 757
- Ulvestad, J. S., Antonucci, Robert R. J., & Barvainis, R. 2005, *ApJ*, 621, 123
- Urry, C. M., & Padovani, P. 1995, *PASP*, 107, 803
- Véron-Cetty, M.-P., Joly, M., Véron, P., Boroson, T., Lipari, S., & Ogle, P. 2006, *A&A*, 451, 851
- Zamanov, R., Marziani, P., Sulentic, J. W., Calvani, M., Dultzin-Hacyan, D., & Bachev, R. 2002, *ApJ*, 576, L9
- Zamorani, G., et al. 1981, *ApJ*, 245, 357
- Wang, T., Brinkmann, W., & Bergeron, J. 1996, *A&A*, 309, 81
- Wang, T.-G., Dong, X.-B., Zhang, X.-G., Zhou, H.-Y., Wang, J.-X., & Lu, Y.-J. 2005, *ApJ*, 625, L35